

A NOVEL METHOD FOR MEASURING ELASTIC MODULUS OF FOUNDRY SILICATE BINDERS

Philipp Lechner  **Nils Kraschienski and Wolfram Volk**

Chair of Metal Forming and Casting, Technical University of Munich, Walther-Meissner-Strasse 4, 85748 Garching, Germany

Pavel Filippov

Department of Applied Sciences and Mechatronics, University of Applied Sciences Munich, Lothstr. 34, 80335 Munich, Germany

Florian Ettmeyer and Wolfram Volk

Fraunhofer IGCV, Zeppelinstr. 15, 85748 Garching, Germany

Abstract

This article develops a novel method for measuring the elastic modulus of hardened silicate binders for foundry cores. We measured hardened silicate binder within the original dimensions of the binder bridges with a nanoindenter. The influence of varying hardening times and temperatures on the elastic modulus was studied. This work aims at modelling and simulating the microstructure of sand core materials. In order to develop a computational

model, which determines the mechanical properties of inorganically bound sand, one needs to measure these properties for the hardened inorganic binder itself.

Keywords: *elastic modulus of silicate binders, inorganic core materials, microstructure, foundry binders, nanoindentation*

Introduction

In many light metal foundries, organically bound sand cores are slowly being replaced by inorganic sand-binder systems with the aim of making production more ecologically friendly, in order to adjust the casting process to meet the current environmental protection laws. Inorganic sand cores are produced by bonding natural silica sand with silicate binders.^{1,2} One main advantage of casting with inorganic sand cores over using organic core material is the significantly lower amount of hazardous gasses produced during metalcasting.

This can be attributed to the fact that mainly water is emitted by the silicate binders during the process.³ The casting quality is strongly affected by the macroscopic properties of the core material, including the thermal conductivity,⁴ heat capacity and permeability as well as the mechanical strength of the material.

These properties are defined by the underlying microstructure and its characteristics. However, until recently, only a heuristic description of the macroscopic properties of the inorganic binder system could be found. Therefore, back-tracing the impact that the individual constituents of the sand core material and its underlying microstructure have on the mechanical behaviour of the material would greatly improve understanding of the resulting macroscopic properties of the inorganically bound sand cores.

Microstructural Simulation of Mechanical Properties of Sand Core Materials

Schneider et al. proposed a microstructural model for inorganically bound sand core materials. The model is composed of silica sand grains and binder bridges connecting the particles. First, the sand is packed by an algorithm to a pre-defined volume fraction. In the next step,

binder bridges are inserted with mathematical morphological operations. However, the elastic modulus of the inorganic binder agent is still unknown.⁵ Furthermore, the assumption of homogeneous binder properties has to be tested in order to compute elastic properties of sand core materials accurately.

This article will tackle these questions. In order to determine which core production parameters have the greatest impact on the elastic modulus of the binder, these influences will be isolated and varied separately. The main goal is to determine which hardening conditions have to be considered in order to determine the elastic properties of the binder bridges in the simulation.

Influence of Hardening Conditions on Mechanical Properties of Silicate Binders and Inorganic Sand Cores

Most of the published work regarding the mechanical properties of sand core materials only determines the properties of the whole compound, but not the mechanical properties of the silicate binder alone.⁶ Yet some work does exist in which the properties of silicate binders are investigated in a different context than foundry core manufacturing. As sodium silicate, the main ingredient of silicate binders, is a substance with very broad uses, there are various possible applications. For instance, sodium silicate is used as a non-reflective coating material for displays. In this context, hardness and scratch resistance of a thin silicate display coating is studied, using nanoindentation.^{7,8} As, in this instance, the focus is on the scratch resistance of different coatings, the measuring procedure is just a side aspect of this work. Hence, very little information is provided about the measuring and hardening conditions of the silicate. Furthermore, the sodium silicate serves only as a coating material, which makes it highly likely that the results will not be transferable to the simulation of sand core materials.

Nanoindentation

Nanoindentation is an approved and widely used method of measuring the mechanical properties of small volumes of material. In this study, it was used to access the elastic properties of the binder bridges.

Nanoindentation is a variant of the indentation hardness test applied to small volumes of material where displacement is measured in nanometres rather than micrometres or millimetres. The sample surface is indented by a defined force with a body (indenter) that is harder than the tested material. Additionally, the geometry and mechanical properties (Young's Modulus and Poisson's number) of the indenter must be well known.⁹ During the indentation process, displacement and load are recorded continuously.

Once the indentation procedure is complete, the resulting load–displacement curve is analysed by the device software. From this curve, numerous material parameters, such as hardness and indentation modulus,^{10,11} can be calculated.

Materials and Methods

The mathematical model used to calculate the elastic modulus is based upon an assumption of an ideally flat surface. Real surfaces, however, are never absolutely flat but rough to a certain degree. In order to keep the indentation depth uncertainty under 20%,⁹ the following criterion can be applied:

$$h \geq R_a \quad \text{Eqn. 1}$$

where h is the indentation depth and R_a the arithmetic average roughness of the examined surface. This criterion, however, is difficult to meet, since the roughness of the binder bridges in question is unknown. Furthermore, the hardened binder bridges contain pores. The resulting uncertainty will be met with a suitable sample size.

Measuring System

Requirements to the Measurement System

In order to access the mechanical properties of the binder bridges, a suitable method has to be capable of measuring very small material volumes. Combined with the high lateral positioning accuracy of nanoindentation, the binder bridges can be easily navigated and indented separately from the sand grains.

Unlike the conventional indentation hardness test, no optical measurement of the remaining indent is necessary. All material parameters are calculated from the load–displacement curves, which can be acquired with a very high degree of precision. This is essential for measuring small features like binder bridges, since the original indent is too small to be measured optically.

Description of the Nanoindentation Systems Used

In this study, two nanoindentation systems were used, since they are equipped with different measuring tips:

- “Picodentor HM500” manufactured by Helmut-Fischer GmbH, equipped with a Vickers tip
- “Nanotest Vantage” manufactured by Micro Materials Limited, equipped with a spherical tip

Typically, elastic modulus is measured with a Vickers or Berkovich tip which is as sharp as possible. However, the heterogeneous and porous character of the measured binder

system made a spherical tip necessary for one type of specimen. The measuring system used for each specimen will be stated with the specific description of each experiment in Sects. 2.3 and 2.4.

The basic operation principle of the “Picodentor HM500” is shown in Figure 1. First, the measuring head is placed upon the sample surface to minimise device compliance. Then, the indenter is moved towards the sample. Once the surface is detected, the actual measurement is started. In the “Nanotest Vantage”, the sample is moved to the towards the indenter, which allows a bigger range of sample dimensions.

The force is generated with high precision via an electromagnetic induction coil. The indentation depth is measured via eddy current probe. Both parameters are measured constantly during a single indentation. A programmable XY table allows the sample to be positioned automatically.

With the automated XY table, the nanoindenters also allow a grid matrix to be set up, by defining the number of indents and the distance between them. The grid is then executed automatically, and the results can be combined to create a property map of the sample surface.

To reduce ground vibrations, the “Picodentor HM500” is installed on an active piezoelectric vibration cancellation system. The complete system is placed within a sound insulation casing in order to minimise acoustic influences. These measures are required to allow appropriate measurements at very low loads.

The “Nanotest Vantage” is placed on a passive damping system. The casing is also temperature controlled, to minimise the effect of temperature oscillations.

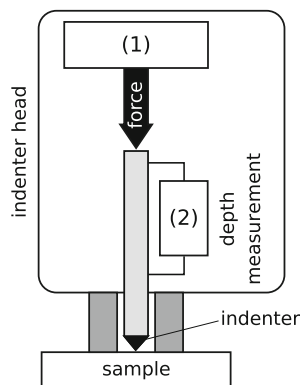


Figure 1. Simplified representation of the measuring head of the nanoindentation tool “Picodentor HM500” according to the device supplement information. (1) Force generation via electromagnetic induction, (2) indentation depth measurement via eddy current probe.

Measurement Procedure

The typical nanoindentation procedure consists of the following phases, as illustrated in Figure 2:

1. Surface approach and contact
2. Load phase
3. Hold at maximum load to allow for occasional creep
4. Unload phase
5. Hold near zero load to compensate for temperature influences (optional)

In the first step, the indenter and the sample are slowly brought together (displacement only, no load change) until they make contact. Then, the indenter is pushed into the surface in a force-controlled manner, until the designated load is reached. In this step, the sample is deformed elastoplastically. When the maximum load is reached, a hold phase at constant load can be introduced to allow the material to creep. In the last step, the indenter is withdrawn from the surface, while the sample recovers elastically. This purely elastic recovery makes it possible to determine the elastic modulus of the sample.

Calculation of Elastic Modulus

The calculation of the elastic modulus was performed according to the method of Oliver and Pharr,¹² which is based on the original work of Doerner and Nix.¹³ The elastic modulus of the diamond indenter E_i is 1140 GPa and the corresponding Poisson’s number ν_i is 0.07. The Poisson’s number of the sample ν_s must also be known in order to calculate the real elastic modulus of the material. Since no public work is available on the Poissons’s number

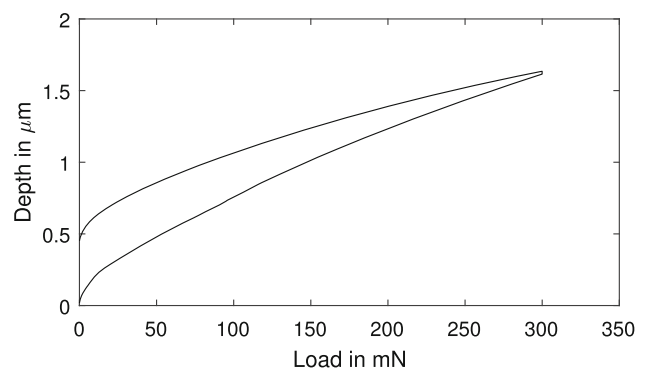


Figure 2. Exemplary load–displacement curve of a binder bridge. The measurement is started at zero load and displacement; as the load rises so does the displacement (depth) until the maximum load of 300 mN is reached. After a brief hold time, the load is withdrawn. The elastic properties are determined on the basis of the unload part of the curve.

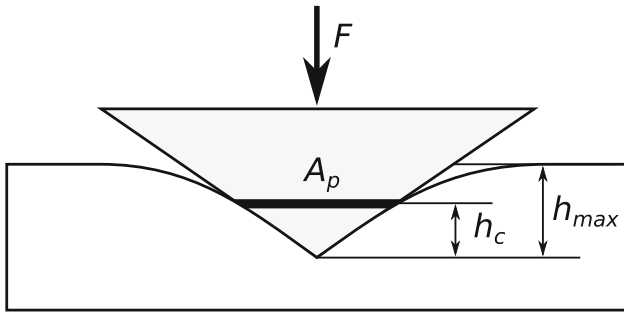


Figure 3. Schematic representation of the indentation including specific values necessary for the calculation of nanoindentation parameters, adapted from the literature.⁹

of silica binder, the Poisson's number of amorphous silica $\nu_{\text{SiO}_2} = 0.168$ is used.¹⁴ Thus the elastic modulus can be calculated as:

$$E_{\text{IT}} = \frac{1 - (\nu_s)^2}{\frac{1}{E_r} - \frac{(1 - \nu_i)^2}{E_i}} \quad \text{Eqn. 2}$$

The reduced modulus E_r is calculated on the basis of contact stiffness S (determined numerically from the unload part of the load-displacement curve) and the projected area at the contact height $A_p(h_c)$ (Figure 3):

$$E_r = \frac{\sqrt{\pi} \cdot S}{2\sqrt{A_p(h_c)}} \quad \text{Eqn. 3}$$

Sand Microsection: Measuring Binder Bridges in the Sand-Binder Context

Description of the Testing Method

Since the mechanical properties of inorganic sand cores are very sensitive to changes in the hardening conditions,^{3, 15} it is desirable to measure the silicate binder directly in the sand-binder microstructure, which is produced by the core blowing process. This guarantees that the hardening conditions are as close as possible to the cores that are supposed to be simulated. However, as Figure 4 shows, the binder bridge dimensions are usually smaller than the diameter of the bound sand particles, which makes them inaccessible for most measuring techniques. Furthermore, the surface is rough. This makes it necessary to use microsections for the nanoindentation measurements.

Specimen Preparation

The inorganically bound sand core material used for the specimens was blown on a Loramendi SLC2-25L with water-cooled shooting head, shooting nozzles and sand funnel. The core box is heated and a hot air drying mechanism is available. The temperature of the tool was set to 155 °C and the temperature of the hot air to 220 °C. A



Figure 4. Binder bridge under the microscope.

ceramic "Cerabeads 400" sand was used (Hüttenes-Albertus Chemische Werke GmbH, Düsseldorf, Germany). It was bound with an inorganic binder system containing 2 wt% (relative to sand mass) Innotec EP4158 and 1.6 wt% Innotec TC4500 (ASK-Chemicals, Frechen, Germany). After the core blowing, the specimens were stored in a desiccant based on a silica gel. Subsequently, the sand core material was polished with ethanol-based substances to avoid chemically damaging the binder bridges with water-based polishing.

To take the measurements, the Nanotest Vantage system was used and the following settings were chosen:

- Spherical tip with a 10 μm radius
- Maximum load 50 and 100 mN
- Loading time 20 s
- Unloading time 10 s
- Dwell time at maximum load 30 s
- 60 s temperature drift correction post-indentation

A spherical tip was utilised because the assumption was made that a Vickers or Berkovich would be more sensitive to the porous surface resulting from the polishing of the binder bridges. For the same reason, it is desirable to use as much load as possible. The upper force limit is reached when the surface is damaged, which leads to an invalid calculation of the elastic modulus.

Measuring Isolated Binder Droplets

Description of the Testing Method

The test specimen is based on a polished steel disc, spray-coated with silicate binder. The small droplets on the steel disc can be tested regarding their elastic properties using nanoindentation. The disc serves as a carrier for the binder droplets in the nanoindentation test. In order to achieve valid test results, one side of the steel disc was sanded and polished to a minimal grain size of 3 μm. The steel disc was



Figure 5. Mirror-finish-polished specimen (left) and sodium silicate binder sprinkled specimen after hardening (right).

polished until it had a mirror finish. The surface roughness ranges below the binder droplets measured, and the binder droplets could be assumed to be flat on their bottom side. After surface preparation, the specimen is lightly sprinkled with liquid sodium silicate binder using a standard spay pistol. It is essential that no closed coating film is created, but individual binder droplets can be distinguished. After the spraying procedure, the binder is hardened in an oven with varying curing parameters. Figure 5 shows both a polished specimen ready for sprinkling and a sprinkled and hardened specimen. Figure 6 shows a microscope image of the binder droplets under the “HM 500” microscope. For the nanoindentation, the following settings were chosen for the Picodentor HM 500:

- Vickers tip
- Maximum load 50 mN
- Loading time 50 s
- Unloading time 50 s
- Dwell time at maximum load 5 s

Experimental Results

Experimental Results for Measuring Binder in Its Microstructure Context

As stated in Sect. 2, the elastic modulus can be measured locally with one indent, but it is also possible to program a grid with multiple measuring points. This was done for the binder bridges shown in Figure 7. The grid area is marked as well. The coloured scale of the heatmap shows E_{IT} in the grid. In order to show the differences in elastic modulus of the binder bridges more clearly, the colour bar was limited to 80 GPa. The measuring points used for the heatmap are marked with a cross in a circle. Between those indents, the colours are interpolated linearly.

The binder bridges and the sand particles are clearly distinguishable, however distinguishing the embedding material and the binder bridges is more difficult. The elastic modulus of the embedding is below 10 GPa, but there is no discrete boundary between the binder and the embedding. This is due to the dimensions of the indents, both in depth and in area. Additionally, the embedding is able to fill the porous binder structure in the peripheral area of the binder bridge. This leads to a continuous transition in

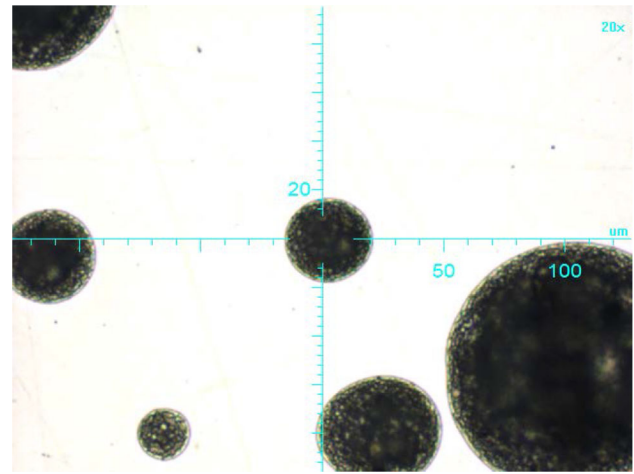


Figure 6. Binder droplets under the nanoindenter (“HM 500”) microscope.

elastic modulus from binder to embedding. For a quantitative analysis, the authors chose indents with the highest certainty of being pure binder (marked in red with a circle). The results are shown in Table 1.

Clearly, the results are not independent of the test load, which would be the case for an ideal material, such as fused silica. The higher testing force leads to a bigger contact area with the porous surface, resulting in the higher and more realistic E_{IT} and a lower standard deviation. This leads to the assumption that a higher testing force is beneficial. However, the testing load could not be raised further, since a higher force would lead to surface damages on the binder bridges.

Further problems arise, when a larger number of data sets are necessary. The goal is to test the sensitivity of the elastic properties to specific changes in the hardening conditions, which is very important for microstructural simulations. Therefore, a larger sample size has to be considered.

The first problem is that the measurement of a full grid is very time-consuming, since measurements (a) and (b) contain 100 indents and (c) 225 indents with a measuring rate of 20–30 indents per hour.

Second, binder bridges are hard to find in a cross-section of the sand core, since they are very small compared to the sand particles, and so is the probability of them being in the plane of the cross-section. There are some in every microsection, but the process of finding the ones suited for nanoindentation is very complex.

These difficulties lead to the necessity for another type of specimen that is suited for larger measurement series and follows the same chain of cause and effect, in order to tackle wide parameter variations.

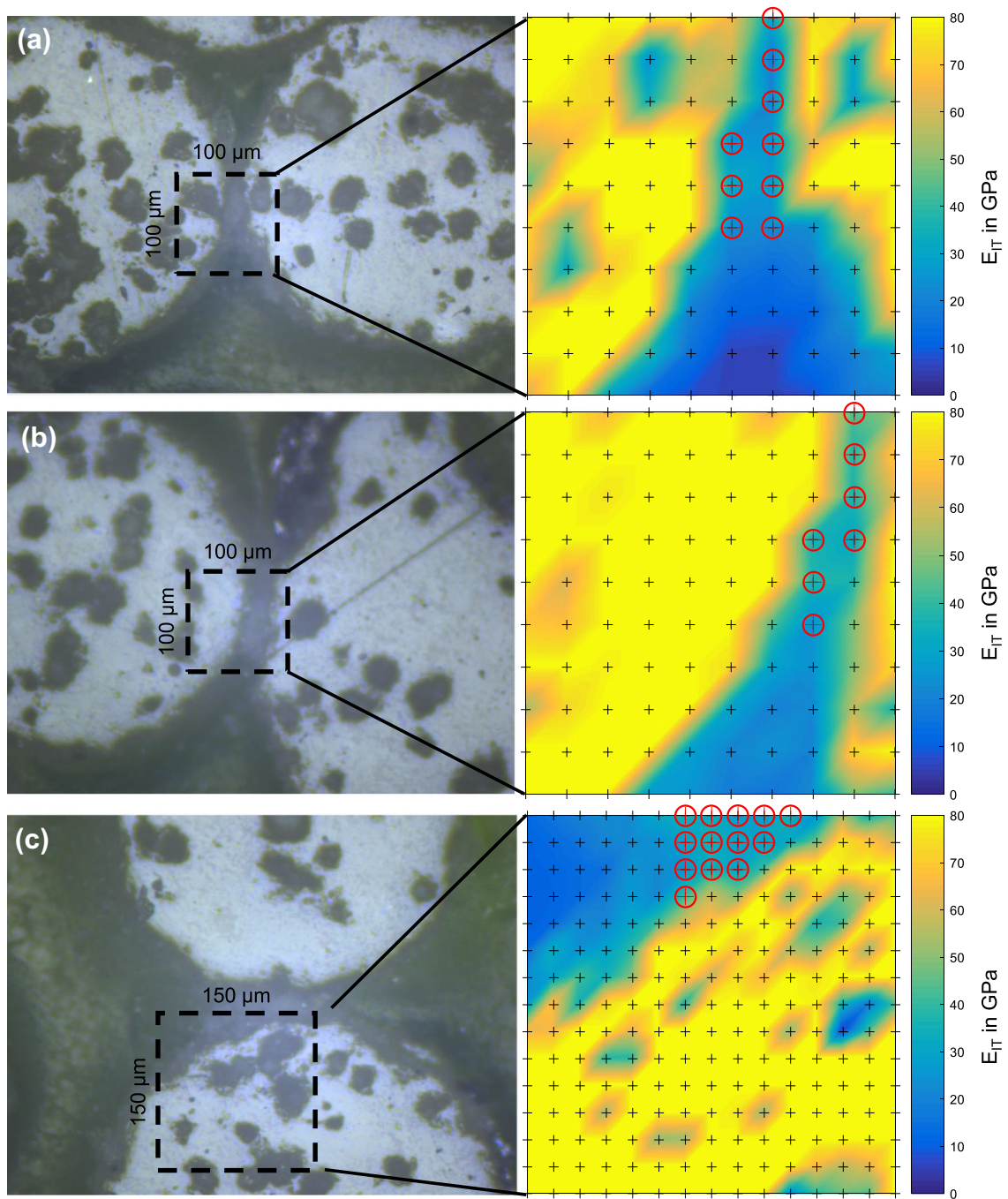


Figure 7. Measured elastic modulus of three binder bridges. For measurements (a,b) a 10×10 grid ($10 \mu\text{m}$ between indents) was utilised, for (c) a 15×15 grid. (a) was performed with 50 mN testing force; (b, c) were performed with 100 mN. The data are tabulated in Table 1.

Table 1. Measurement of Elastic Modulus for Different Binder Bridges with 50 mN and 100 mN Testing Force

Binder bridge	(a)	(b)	(c)
Testing load in mN	50	100	100
Elastic modulus in GPa	24.74	35.41	31.81
Standard deviation in GPa	4.58	6.35	4.32

Measuring the Isolated Binder

In order to measure a large number of data points efficiently, it is desirable to produce specimens made purely of binder, without the sand component. Furthermore, the specimens should be similar in size to the original binder bridges to avoid scaling effects, which lead to different hardening conditions.

Varying Core Blowing Parameters

In this section, a parameter study is performed to determine the impact of the most important core blowing parameters on the elastic properties of the binder:

- The temperatures of the tool and the hot air
- The curing time in the tool
- The binder fraction in the sand core material

Since the specimens are cured in an oven, the core blowing temperatures are represented by the oven temperature. Analogously, the curing time in the tool translates to different oven times. The binder fraction in the core material influences the number and size of the binder bridges with the extreme case of a full binder matrix around the sand particles. For this reason, different droplet sizes are measured and varied as well.

Size Dependency

To analyse the size dependency of the elastic properties of the inorganic binder, different droplet sizes were chosen for nanoindentation. Since the size of binder bridges is determined by various influences, such as particle size and form, binder amount and binder viscosity, a range of droplet diameters between 30 and 80 μm were measured. The results are shown in Figure 8.

Due to the heterogeneous and porous character of the binder, the standard deviations are comparatively high, since the indentation point hits either an additive particle or waterglass.

With respect to the standard deviation, the droplet size has no significant influence on the reduced elastic modulus of the binder. The measured values range from 41 to 46 GPa, with a mean standard deviation of 15.7 GPa over all data points. The specimens were cured for 5 min at 175 $^{\circ}\text{C}$. For further experiments, droplets with diameter of 50 μm were selected under the microscope.

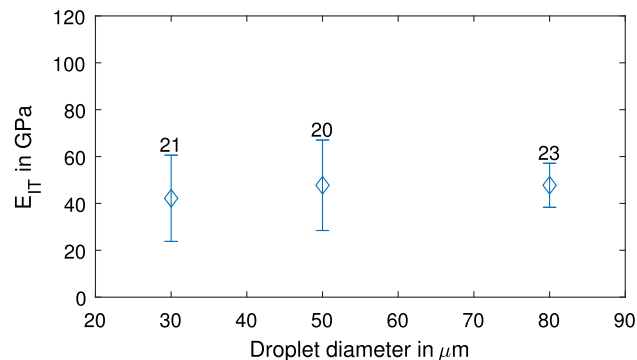


Figure 8. Elastic modulus of silicate binder for different droplet sizes.

Time Dependency

To analyse the time dependency, a broad range of oven curing times have to be chosen, since the curing time with direct contact to the hot tool during the core blowing process cannot be compared directly to the time in the preheated oven. However, the relative chain of cause and effect is assumed to be correct.

Oven times between 5 min and 30 min were chosen. The other curing parameters were 145 $^{\circ}\text{C}$ and 50 μm droplet size. A rising elastic modulus between 44.3 and 67.1 GPa can be stated for an increasing curing period, as shown in Figure 9. The mean standard deviation is 17.3 GPa over all data points.

Temperature Dependency

In order to determine the influence of the curing temperature, 145 $^{\circ}\text{C}$ and 175 $^{\circ}\text{C}$ were chosen as oven temperatures, which are both typical for the core blowing process. Both sets of specimens were cured in the oven for 5 min. The data points are 43 GPa at 145 $^{\circ}\text{C}$ and 46 GPa at 175 $^{\circ}\text{C}$, as shown in Figure 10. Similar to the question of size dependency, the difference is not significant compared to

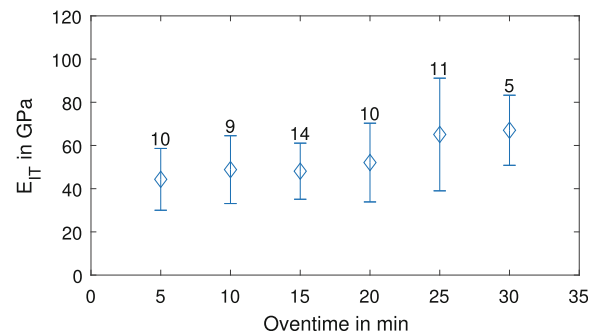


Figure 9. Elastic modulus of silicate binder for different hardening times.

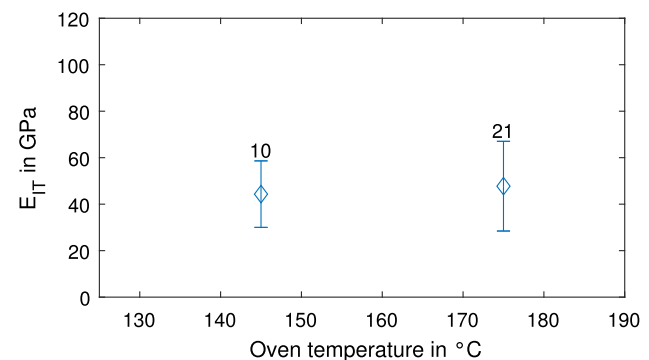


Figure 10. Elastic modulus of silicate binder for different hardening temperatures.

the mean standard deviation of 16.8 GPa over all data points.

Discussion

Both methods offer different advantages. Measuring inside the sand-binder microstructure leads to a direct measurement of a binder bridge, while the droplet method offers only relative gradients for changes in production parameters. However, the droplet method is more effective, when considering the necessary effort. The droplets do not have to be polished for measurement, and they can be selected efficiently under the microscope. In contrast, measuring real binder bridges is a complex process. The specimens have to be polished, and it is time-consuming to find binder bridges which are suited for indentation. A combination of both methods is advised for most problems. Studying the relative influence of varying core curing parameters like tool temperature and time can be achieved with the droplet method, and the results can be validated absolutely with few measurements of binder bridges.

The main goal of this work is to determine the elastic modulus of silicate binders for microstructural simulations of inorganic sand core materials. From a technical point of view, the most important question is:

Which core blowing settings influence the elastic properties and have to be accounted for? This can be answered with the results from Sect. 3.2. While the absolute elastic modulus differs from the results from Sect. 3.1, the relative chain of cause and effect is valid, since the hardening mechanism, a condensation reaction,³ is very similar in the oven and the core blowing tool. Furthermore, it is likely that the elastic modulus measured directly from binder bridges would rise further with higher testing loads. Based on the results from Sect. 3.2, only the tool time has to be considered for future studies of the elastic modulus. Furthermore, when evaluating the weightiness of these influences, one has to consider the effect of the binder's elastic properties on the simulation. Scheider et al. assume a wide range of elastic moduli between and 10 and 100 GPa and show that the effective elastic modulus of the sand-binder compound follows a square-root-shaped function for a rising binder elastic modulus. Thus, the influence of the binder on the microstructure diminishes with an increasing elastic modulus. When applying the model of Schneider et al. with the elastic moduli determined in this article,⁵ the effective elastic modulus of the sand-binder compound is already saturating.

This justifies neglecting the small influences of binder bridge size and curing temperature, which saves a lot of modelling and experimental effort in future, since both effects would have to be modelled in the microstructure.

For simulating purposes, it will be necessary to study the inorganic binder system used for different curing times.

Conclusion

Two novel methods have been developed to measure the elastic modulus of hardened silicate binders with nanoindentation. The first method measures binder bridges directly in the sand-binder compound. The second method utilises binder droplets on steel carriers, which are cured in an oven. Measuring the elastic modulus with binder droplets is more efficient and allows to study the chain of cause and effect when varying production parameters. However, the curing of the binder possibly differs from the original curing within the core blowing machine. Hence, the absolute values of the measurement have to be validated with direct indentation of binder bridges within the original microstructure.

Both methods were used to measure the elastic properties of a binder system in the sand microstructure itself, and for a parameter variation to determine the influence of typical core blowing parameters. The following parameters were varied to study the influence on the elastic modulus of the silicate binder:

- The diameter of the droplets, which relates to the size of the binder bridges and the binder fraction in the sand.
- The curing temperature and time, which relate to the tool temperature and time, respectively.

The diameter of the droplets and the curing temperature had no significant effect, while the curing time increases the elastic modulus, when rising itself.

Recent simulations of the sand-binder microstructure have studied the effect of the binder's elastic modulus on the macroscopic elastic modulus of the sand-binder compound, but lacked a measured value for it.⁵ With the knowledge obtained in this article, they can be performed with a full set of material parameters to further advance the knowledge of the mechanical behaviour of inorganically bound core materials.

Acknowledgements

This research was supported by DFG Projects VO 1487/16-1 and VO 1487/37-1.

REFERENCES

1. W. Tilch, U. Nitsch, Archives of Foundry **2**(3), (2002). <http://www.afe.polsl.pl/index.php/pl/1539/giesserei-und-umwelt-wege-zurnachhaltigen-guss-stueckfertigung.pdf>

2. J.T. Fox, F.S. Cannon, N.R. Brown, H. Huang, J.C. Furness, *Int. J. Adhes. Adhes.* **34**, 38 (2012)
3. H. Polzin, *Inorganic Binders: For Mould and Core Production in the Foundry* (Schiele & Schön, Berlin, 2014)
4. R. Rajkolhe, J. Khan, *Int. J. Res. Adv. Technol.* **2**(3), 375 (2014)
5. M. Schneider, T. Hofmann, H. Andrä, P. Lechner, F. Ettemeyer, W. Volk, H. Steeb, *Int. J. Solids Struct.* (2018). <https://doi.org/10.1016/j.ijsolstr.2018.02.008>
6. B. Griebel, D. Brecheisen, R. Ramakrishnan, W. Volk, *Int. J. Metalcast.* **10**(4), 524 (2016)
7. Q. Zhao, M. Guerette, L. Huang, *J. Non-Cryst. Solids* **358**(3), 652 (2012)
8. J. Němeček, V. Šmilauer, L. Kopecký, *Cement Concr. Compos.* **33**(2), 163 (2011)
9. DIN Deutsches Institut für Normung e. V. *Metallische Werkstoffe – Instrumentierte Eindringprüfung zur Bestimmung der Härte und anderer Werkstoffparameter – Teil 1: Prüfverfahren* (2015)
10. A.C. Fischer-Cripps, *Nanoindentation*, 3rd edn., Mechanical Engineering Series (Springer, New York, 2011)
11. H. Biermann, L. Krüger, *Moderne Methoden der Werkstoffprüfung*, 2nd edn. (Wiley, Hoboken, 2015)
12. G.M.P.W.C. Oliver, *J. Mater. Res.* **7**(6), 1654 (1992)
13. M.F. Doerner, W.D. Nix, *J. Mater. Res.* **1**(04), 601 (1986)
14. W. Pabst, E. Gregorova **57**, 167 (2013)
15. C. Wallenhorst, *Giesserei* **3**, 34 (2008)